Excess of low frequency vibrational modes and glass transition: A molecular dynamics study for soft spheres at constant pressure

Hugo M. Flores-Ruiz[1] and Gerardo G. Naumis[2,a)]
[1]*Departamento de Física-Química, Instituto de Física, Universidad Nacional Autónoma de México (UNAM), Apartado Postal 20-364, Distrito Federal, 01000 Mexico, Mexico*
[2]*Facultad de Ciencias, Universidad Autónoma del Estado de Morelos, Av. Universidad 1001, Colonia Chamilpa, Cuernavaca, 62210 Morelos, Mexico*

(Received 22 April 2009; accepted 18 September 2009; published online 15 October 2009)

Using molecular dynamics at constant pressure, the relationship between the excess of low frequency vibrational modes (known as the boson peak) and the glass transition is investigated for a truncated Lennard-Jones potential. It is observed that the quadratic mean displacement is enhanced by such modes, as predicted using a harmonic Hamiltonian for metastable states. As a result, glasses loose mechanical stability at lower temperatures than the corresponding crystal, since the Lindemann criteria are observed, as is also deduced from density functional theory. Finally, we found that the average force and elastic constant are reduced in the glass due to such excess of modes. The ratio between average elastic constants can be approximated using the 2/3 rule between melting and glass transition temperatures. © *2009 American Institute of Physics*.
[doi:10.1063/1.3246805]

I. INTRODUCTION

Glass formation is not yet fully well understood.[1–4] In spite of this, our civilization has been making glasses since thousands years ago. For example, window glasses are made following empirical recipes, and only very recently rigidity theory (RT) provided the first theoretical explanation of such recipe.[5] Almost all glasses present an excess in the density of low frequency vibrational modes[6] (LFVMs) when compared with crystals. One example is the boson peak[6] and the other is the floppy mode contribution.[7,8] While there is no consensus about the nature of the boson peak,[9] the appearance of floppy modes can be successfully explained by the Phillips–Thorpe constraint theory.[10,11] Historically, both anomalies were considered as different phenomena. More recently, there are clear indications that point to the fact that there is a certain commonality between the approach due to Phillips[10] and Thorpe,[11] in which chemical composition is the key variable, and the conventional mode softening approaches to the glass transition at constant composition.[12]

In fact, floppy modes are due to the low coordination of the system, in which the number of constraints (N_c) due to bonding is less than the number of degrees of freedom ($3N$ where N is the number of atoms). Systems where $N_c=N-5$ are known as isostatic, where 5 is due to the counting of the trivial degrees of rotation and translation of the system.[13] It has been even possible to observe a glassy phase in which atoms are able to self-organize in isostatic networks to reduce stress.[14–16] Recently, there has been a wide support to the idea that rigidity plays a role in the field of jamming transitions.[17] Jamming is the process by which some materials, such as foams, collections of grains, and other complex fluids, become rigid with increasing density due to the crowding of the constituent particles that block particle movements. Such behavior can be explained in terms of the number of contacts between particles, as it happens in rigidity. It is believed that the glass and jamming transitions are just different manifestations of a generalized phase diagram.[18] Furthermore, the nature of the boson peak has been traced back to the low coordination of a network[17] and identifies the frequency of the boson peak as the frequency above which the onset of the soft modes (obtained from constraint counting) is observed.

Although LFVM anomalies are present in all glasses, most of the theories do not give a special importance to this observation.[19] Mode coupling certainly cares about LFVM;[6] however, it seems that the connection with the excess of modes has not been studied thoroughly. Such lack of attention is surprising since LFVM are fundamental to the stability of a solid, as suggested by Peierls many years ago.[6] In a series of previous papers,[20–22] we have shown that the anomalies in the LFVM can determine the glass transition temperature (T_g) as a function of the chemical composition for chalcogenide glasses, as well as the thermal relaxation properties.[23] The key idea was to combine RT with the Lindemann criteria for the mean quadratic displacement.[20] As a result, one can obtain the well known empirically modified Gibbs–DiMarzio law, where the constants that are usually fitted from the experiment have a precise meaning from a physical point of view.

Also, there are other works that relate hard spheres,[24–26] colloids,[27,28] and soft spheres[29–31] with rigidity and anomalies in LFVM. Thus, it is tempting to explore if the observations made for chalcogenide glasses in Ref. 20 are observable in computer simulations of simple systems. In this article we explore the relationship between the mean qua-

a)Electronic mail: naumis@fisica.unam.mx. On leave from: Departamento de Física -Química, Instituto de Física, Universidad Nacional Autónoma de México (UNAM), Apartado Postal 20-364, 01000, México, Distrito Federal, Mexico.

dratic displacement and the excess of modes for soft sphere glasses using molecular dynamics at constant pressure and temperature. A comparison to the corresponding crystalline phase is also presented. The mean quadratic displacement is an interesting quantity since it provides a rough estimation of the mechanical stability of the network, as well as the time scales involved in the problem.[13,20] Notice that we prefer to use constant pressure, instead of the usual *NVT* ensemble in order to obtain a more realistic comparison to experimental situations. Furthermore, our soft sphere glasses were prepared by using jammed states of hard spheres since as we show here, they can provide local energy minima. Although there is some discussion about the use of jammed states in the context of Lennard-Jones glasses, it is worthwhile mentioning that it is believed that dense supercooled liquids are close to jammed states.[17] According to Wyart,[17] such conclusion is a result of the following argument. Consider two jammed states with packing fraction $\phi_a < \phi_b$ and a supercooled liquid near state a with packing fraction ϕ such that $\phi < \phi_a$. Thus, the free volume per particle in the liquid state goes as $\phi_a - \phi$. If p_a is the probability for the liquid to have a as a jammed state, we have that[17] $p_a/p_b = [(\phi_a - \phi)/(\phi_b - \phi)]^N$, where N is the number of atoms. The higher the packing, the more dense jammed states are favored. A similar conclusion can be reached from the fact that the entropy difference between jammed and crystalline states is given by[32]

$$\Delta S = Nk_B - Nk_B \ln(\varepsilon/\varepsilon_0), \tag{1}$$

where k_B is the Boltzmann constant, ε is the free volume referenced to its dynamic random-close-packing value, and ε_0 is the minimum value of the free volume. The first term in the previous equation is the communal entropy, which accounts for the entropy difference between a fluid and a solid.[32] As a result, dense jammed states reduce communal entropy by the factor $Nk_B \ln(\varepsilon/\varepsilon_0)$.

The outline of this paper is as follows. In Sec. II we give a brief review of the relationship between low frequency mode anomalies and the mean quadratic displacement. In Sec. III we present the details of the simulation, while the results are presented in Sec. IV. Finally, in Sec. V we give the conclusions.

II. MEAN QUADRATIC DISPLACEMENT AND LOW FREQUENCY MODES

A solid exists because it is stable against thermal phonon fluctuations. Such effect is roughly encoded in the mean quadratic displacement $\sqrt{\langle u^2(T)\rangle}$ of the atoms.[22] In crystals, this leads to the Lindemann criteria,[6] which provide a simple estimate of the melting temperature (T_m). The criteria establish that melting occurs when $\sqrt{\langle u^2(T)\rangle}$ is at least 10% (usually around 15%) of the atomic spacing a. There are experimental evidence that these criteria are applicable to glasses.[33–37] In Ref. 22, we argue that the criteria are valid because a glass is in a local minimum of the energy landscape (also known as inherent structures or basins[38]). Inside the minimum, the atoms are oscillating around equilibrium positions.[38] This means harmonic oscillations.[38] A clear proof of this is the well known experimental fact that the specific heat (C_p) of glasses differs only slightly from the Dulong–Petit law[39] near T_g. Using a harmonic Hamiltonian for the metastable state, the mean quadratic displacement is given by[22]

$$\langle u^2(T)\rangle \approx \frac{3k_BT}{\langle m\rangle}\int_0^\infty \frac{g(\omega)}{\omega^2}d\omega, \tag{2}$$

where $g(\omega)$ is the density of vibrational states at frequency ω and $\langle m\rangle$ is the average mass of the atoms in the system.[22] For example, in a binary compound of the type A_xB_{1-x}, $\langle m\rangle = (1-x)m_A + xm_B$, where m_A and m_B are the masses of each kind of atom. This formula shows what Peierls understood for crystals: the LFVM is fundamental due to the $1/\omega^2$ factor which tends to amplify the effects of $g(\omega)$ when $\omega \to 0$. For crystals, the reduced density of states $g(\omega)/\omega^2$ is a constant due to the Debye law. In glasses, $g(\omega)/\omega^2$ presents a peak in addition to the constant Debye value, and thus an excess in $\langle u^2(T)\rangle$ is also expected. As a consequence, glasses are less stable when compared with the crystal, and then the liquid is found at a lower temperature. To compare with the Lindemann criteria, we can divide $\langle u^2(T)\rangle$ by a^2 and use the density $\rho^{2/3}$ to obtain

$$\frac{\langle u^2(T)\rangle}{a^2} \approx \frac{3\rho^{2/3}k_BT}{\langle m\rangle}\int_0^\infty \frac{g(\omega)}{\omega^2}d\omega, \tag{3}$$

where the second inverse moment is defined as

$$\langle \omega^{-2}\rangle = \int_0^\infty \frac{g(\omega)}{\omega^2}d\omega. \tag{4}$$

Yet we can use a second independent approach to point out the importance of LFVM to the glass transition temperature. By using density functional theory to estimate the free energy barrier of supercooled liquids, it is possible to show that the viscosity $\eta(T)$ at a certain temperature is given by[40]

$$\ln\ \eta(T) \approx \ln\ \eta_0 + \frac{3r_0^2}{4\langle u^2(T)\rangle}, \tag{5}$$

where η_0 is the typical value of the viscosity in the liquid phase and r_0^2 is a constant that depends on the system. For a truncated Lennard-Jones potential,[40] $r_0 \approx 0.38\sigma$ (where σ is a parameter defined below), while for a Ni–P mixture is around 0.5σ. Usually, T_g can be defined as the temperature at which $\eta \approx 10^{13}$ P. Inserting this condition into Eq. (5), we get

$$\frac{\langle u^2(T_g)\rangle}{r_0^2} \approx \frac{3}{4(13-y)\ln 10} \approx \frac{0.033}{13-y}, \tag{6}$$

where y is an exponent defined as $\eta_0 = 10^y$. For typical fluids,[40] $y \approx 3$ from where we obtain

$$\frac{\langle u^2(T_g)\rangle}{\sigma^2} \approx 0.0125, \tag{7}$$

and thus $\sqrt{\langle u^2(T_g)\rangle} \approx 0.11\sigma$, which is close to the value obtained from the Lindemann criteria. Notice that the simple derivation presented here provides a general explanation for the fact that glasses follow in a rough way the Lindemann

criteria.[33] It also provides a relationship between glass transition and LFVM when combined with Eq. (3). In Sec. IV we corroborate the validity of this hypothesis for soft sphere glasses. Before doing that, let us present in Sec. III the details of the simulation.

III. MOLECULAR DYNAMICS SIMULATION AND GLASS PREPARATION

In all of the simulations, we have used a truncated Lennard-Jones potential where only the repulsive part is kept,

$$\Phi(\mathbf{r}_1, \ldots, \mathbf{r}_N) = \begin{cases} \epsilon\left(\frac{\sigma}{r_{ij}}\right)^{\beta} & \text{if } r_{ij} \leq \sigma, \\ 0 \text{ in any other case,} \end{cases} \tag{8}$$

where $r_{ij}=\|\mathbf{r}_i-\mathbf{r}_j\|$, $\mathbf{r}_j$ is the position of the j particle, and ϵ is a constant energy. The simulations were made using molecular dynamics at constant pressure and temperature. The equations of motions were solved with the standard predictor-corrector algorithm in a cubic box with periodic boundary conditions. The units of mass, length, time, pressure, and temperature are m, σ, $\tau=\sigma\sqrt{m/\epsilon}$, ϵ/σ^3, and ϵ/k_B, respectively, with k_B being Boltzmann's constant. The parameter of the potential was chosen to be $\beta=12$. The simulations were performed in boxes containing $N=864$ and $N=500$ particles.

Since the aim of this paper is to compare measurements done on a glass with the ones done on a crystal, we prepared systems with different initial configurations. The starting configurations (at zero pressure and zero temperature) were a face-centered cubic (*FCC*) for the crystal and *jammed* states for the glasses. The jammed states were produced via the executable codes from Donev *et al.*[41] The atoms in the crystal were of the same size as in the glass with diameter $d=\sigma$. The same radius was chosen for hard and soft spheres since, as shown in Appendix A, states prepared in this way are in a local energy minimum for a soft spheres potential. The initial configurations were heated from a solid to fluid state. At the same time, we got enough information to compute the mean square displacement $\langle u^2(T)\rangle$ and the velocity autocorrelation function $\langle \mathbf{v}(t)\cdot\mathbf{v}(0)\rangle$. This correlation was used to obtain the density of vibrational states $g(\omega)$ from[42]

$$g(\omega) = \frac{1}{3NTk_B}\int_0^{\infty} \langle \mathbf{v}(t)\cdot\mathbf{v}(0)\rangle e^{i\omega t}dt \tag{9}$$

and the diffusion constant D,

$$D = \frac{1}{3}\int_0^{\infty} \langle \mathbf{v}(t)\cdot\mathbf{v}(0)\rangle dt. \tag{10}$$

IV. RESULTS

The first step to investigate the glasses and crystals used for the study was to build a diagram of the studied configurations, as shown in Fig. 1, which contains the temperature and packing fraction (ϕ). The triangles correspond to systems obtained by heating a jammed structure, while the circles were obtained by heating a FCC. Notice that for $T\rightarrow 0$, ϕ goes to $\phi_c=0.635$, which is the packing fraction of the maximally jammed state for hard spheres.[43] This diagram is very similar to the one reported for a polydisperse Lennard-Jones system,[43] which also behaves as jammed hard spheres in the limit $T\rightarrow 0$. As it happens in Ref. 43, a region to the right of the studied systems in the T-ϕ diagram is not accessible to our simulations, since the pressure needs to be raised a lot, and thus produces a practical limit for the studied systems in the T-ϕ diagram. To characterize our glasses and crystals, we obtained the radial distribution function ($g(r)$), diffusion constant (D), average density ($\langle\rho\rangle$), enthalpy ($\langle H\rangle$), and internal energy at different pressures. As an example, in Fig. 2 we present D as a function of T for one of the used pressures, in this case $P=30.0$. The figure shows the results for a glass and its corresponding crystal. To test the effects of size scaling, we did all the calculations for $N=864$ and $N=500$ atoms.

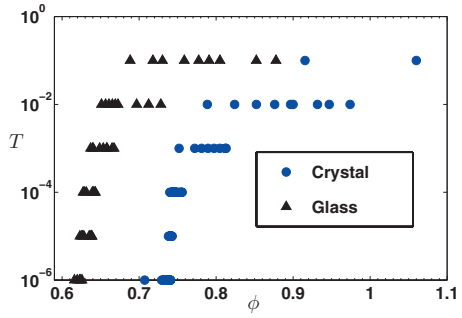

FIG. 1. Diagram that shows the studied systems. The circles were obtained by heating a FCC crystal, while triangles were obtained by heating a jammed structure.

From Fig. 2, we can easily distinguish the solid, supercooled, and fluid phase, since the supercooled fluid departs from the crystalline branch at the melting temperature $T_m\approx 1.8$ (although the melting point is still controversial, see below). The supercooled liquid becomes solid when $D=0$ at $T_g=1.4$ for $N=500$ and $T_g=1.2$ for $N=864$. Figure 3 presents $\langle\rho\rangle$ as a function of T for the same glasses, crystals, and fluids. Clearly, T_m and T_g obtained from this plot are consistent with the ones already obtained in Fig. 2. Notice, how-

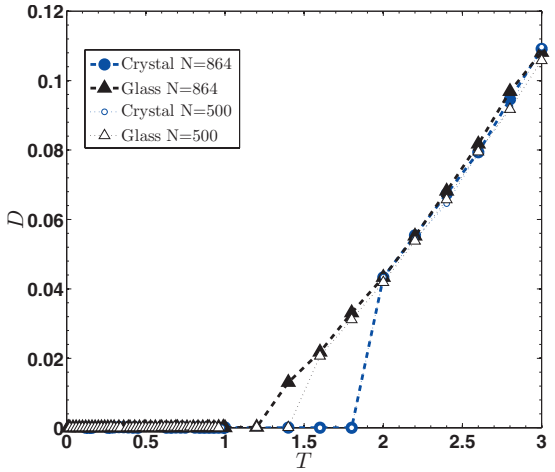

FIG. 2. Diffusion constant as a function of the temperature. The circles are crystals, while the triangles are glasses. Open symbols are for $N=500$ and closed symbols are for $N=864$ atoms. The lines are a guide to the eye.

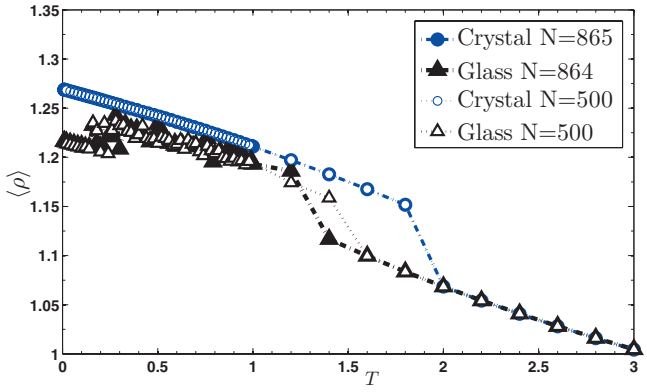

FIG. 3. Density as a function of the temperature. The circles correspond to the crystals, while the triangles are the results for the glasses. Open symbols are for $N=500$ and closed symbols are for $N=864$ atoms. The lines are a guide to the eye.

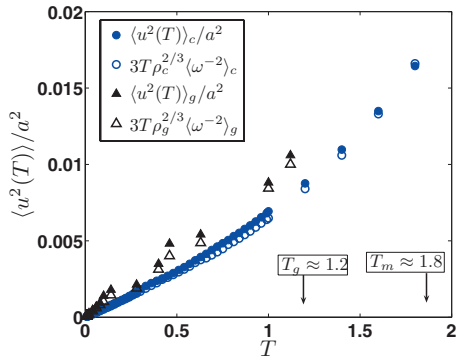

FIG. 4. Normalized mean quadratic displacement as a function of T for the glass (triangles) and crystal (circles) for $N=864$. The closed symbols denoted by $\langle u^2(T)\rangle/a^2$ were obtained directly from the simulation. The open symbols were calculated using Eqs. (9) and (3).

ever, that $\langle\rho\rangle$ fluctuates below T_g. Such behavior is due to different metastable states as we will discuss later. Such jumps are related with the fact that monodisperse Lennard-Jones glasses are weak glass formers.[42] In fact, Lennard-Jones glasses tend to crystallize quite easily. However, since our glasses were obtained by hyperquenching and pressure was kept constant, our solid samples were not crystallized. Similar kind of procedures has been successful in this system.[42] The lack of crystallization was verified using $g(r)$ and by direct inspection of the resulting configurations.

At low temperatures or close to the glass transition, we have found that such behavior is much more stable. It is interesting that the behavior of D and $\langle\rho\rangle$ is very similar for the systems with $N=500$ and $N=864$, even if they were prepared from different jammed states. This fact indicates a mild dependence on the specific chosen jammed state, although this point requires a specific extensive study.

An important observation is that for $N=500$,

$$\frac{T_g}{T_m} \approx 0.78, \tag{11}$$

while for $N=864$,

$$\frac{T_g}{T_m} = 0.67 \approx \frac{2}{3}. \tag{12}$$

This is the very well known empirical 2/3 rule between T_m and T_g. It makes us more confident in the location of the glass transition. It also brings the opportunity for a computer study about the origin of such rule, which is still not understood although it is related with the LFVM anomalies and their localization properties.[22] At other studied pressures, as shown in Table I below, we verified that this rule is changed; however, its value does not depart very much from 2/3, since T_m and T_g have the same tendency with the pressure. Size effects can change the value of T_m and T_g by an estimate of[44] 5%.

TABLE I. Ratio T_g/T_m obtained from the simulations for different pressures and system sizes. The error in the ratio is estimated around 10%.

P	T_g/T_m ($N=500$)	T_g/T_m ($N=864$)
25	0.63	0.63
30	0.78	0.67
35	0.80	0.75
40	0.82	0.67

Once our glasses, crystals, and fluids were characterized, we performed a systematic study of the relationship between low frequency modes, the mean quadratic displacement, and glass transition. To do so, we computed $\langle u^2(T)\rangle$ at constant pressure. For crystals, fluids, and glasses at low temperatures or near T_g, such study is straightforward, since equilibrium is achieved after a few time steps. However, between $T\approx 0.3$ and $T\approx 1.0$, our glasses present jumps between metastable states. Similar effects were observed in Ref. 45 and were called earthquakes. To perform measurements is this region, we did very long runs until the system was in a deep metastable state characterized by a stable $\langle u^2(T)\rangle$ for at least 10^6 time steps.

In Figs. 4 and 5, we present $\langle u^2(T)\rangle/a^2$ as a function of T at $P=30.0$ for a crystal and a glass, where the value of a was obtained from the position of the first peak of $g(r)$. The plots show two interesting features: $\langle u^2(T)\rangle/a^2$ is almost linear in T, and the estimation from density functional theory, which predicts $\langle u^2(T_g)\rangle/a^2\approx 0.012$, is close to the value observed for the glass, since from the simulation we get $\langle u^2(T_g)\rangle/a^2 \approx 0.011$. For the corresponding crystal $\langle u^2(T_m)\rangle/a^2\approx 0.016$.

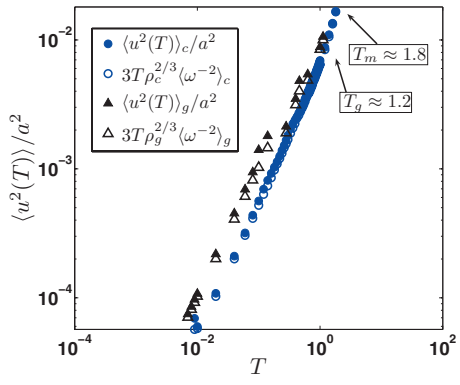

FIG. 5. Log-log plot of the normalized mean quadratic displacement as a function of T for the glass (triangles) and crystal (circles) for $N=864$. Open symbols were calculated using Eqs. (9) and (3), while closed symbols denoted by $\langle u^2(T)\rangle/a^2$ are the results obtained directly from the simulation.

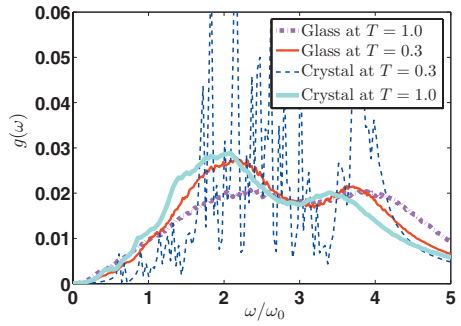

FIG. 6. Density of states as a function of ω for glasses at $P=30.0$ and $T=1.0$ and $T=0.3$ for $N=864$. The corresponding crystals are also shown.

Notice that the Lindemann criteria produce an error of 45% when we compare the crystal with the glass, and thus is a very rough estimation. However, this is in agreement with the fact that fragile glass formers, like our monocomponent fluid, tend to depart from the Lindemann criteria when compared with the corresponding crystal,[37] while strong glass formers are in closer agreement. Furthermore, even the determination of the melting point of Lennard-Jones systems is still controversial,[46] since finite size effects can produce errors around 5%.[44,47] Here we will not further pursue such question. Instead, we will focus on how the features observed in Figs. 4 and 5 are explained by using Eq. (3) and the excess of modes. First, the almost linear dependence of T indicates that the system behaves basically as a harmonic system, as predicted by the T dependence in Eq. (3). From Eq. (3), it seems to be plausible that the excess of low frequency modes can produce an increased $\langle u^2(T)\rangle$. To test this hypothesis, let us calculate $\langle u^2(T)\rangle$ from $g(\omega)$ by using Eqs. (3) and (9). As an example, in Fig. 6 we present $g(\omega)$ for a glass and a crystal at the same temperature and pressure. The glass has an excess of modes in the low frequency region, as has been documented in more detail for Lennard-Jones glasses in Refs. 42 and 48. This is corroborated by looking at $\langle\omega^{-2}\rangle$ for the different glasses and the crystals, as shown in Fig. 7. For all glasses, $\langle\omega^{-2}\rangle$ is always bigger than the corresponding crystal. It is worthwhile mentioning that the ratio between $\langle\omega^{-2}\rangle$ for the crystals and for the glasses is between 1.2 and 2.0, which are values near the predicted 3/2 in Ref. 22.

Figures 4 and 5 present the main point of this article: a

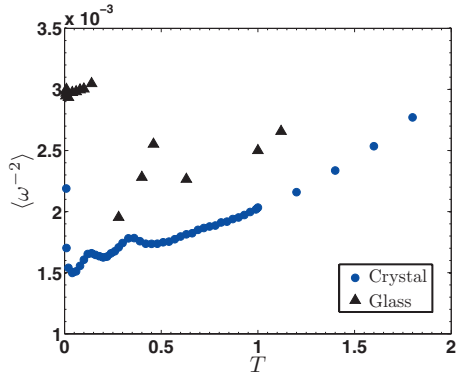

FIG. 7. Second inverse moment of $g(\omega)$ vs temperature for glasses and crystals for $N=864$.

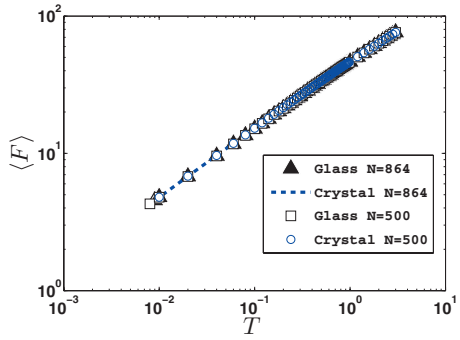

FIG. 8. Average force vs temperature at $P=30.0$ for glasses and crystals of different sizes. Notice how both data sets collapse in the same curve. Two system sizes are presented.

comparison between $\langle u^2(T)\rangle$ obtained directly from the simulation and from the density of vibrational states using Eq. (3), calculated through Eq. (9), in linear and log-log scales. In the case of the crystal, the coincidence is excellent, which means that the harmonic approximation is enough to obtain $\langle u^2(T)\rangle$. For the glass, the slope of $\langle u^2(T)\rangle/a^2$ versus T predicted by Eq. (3) is also very similar to the observed value. This proves a very important point: the harmonic approximation is valid for the glassy phase. Furthermore, we observed that $\langle u^2(T)\rangle/a^2$ is bigger for the glass than the corresponding crystal at the same temperature because of two factors in Eq. (3): one is the increased $\langle\omega^{-2}\rangle$ due to low frequency modes, as shown previously in Fig. 7, and the other is a small correction due to differences in density. This last contribution is around 5% of the total value of $\langle u^2(T)\rangle/a^2$, and thus the main effect is driven by $\langle\omega^{-2}\rangle$. From these simulations, we can conclude that $\langle u^2(T)\rangle/a^2$ is bigger in the glass mainly due to the excess of low frequency modes.

It is also interesting to look at the behavior of the average force defined as

$$\langle F\rangle \equiv \sqrt{\frac{1}{N}\sum_{j=1}^{N}\|F_j\|^2}, \tag{13}$$

where F_j is the force over particle j. Figure 8 shows the evolution of $\langle F\rangle$ as a function of T in a log-log plot. The plot shows two important features. The crystals and the glasses fall nicely in the same curve. Second, the curve is a solid line with slope of 0.485 ± 0.0019 for the solid phase. Thus, $\langle F\rangle \sim T^{1/2}$. Deviations of this law are observed near the glass transition or melting point. In Appendix B, we show that such scaling is expected when the harmonic approximation is valid, since $\langle F\rangle$ is given by

$$\langle F\rangle = \sqrt{3m\langle\omega^2\rangle k_B T}. \tag{14}$$

Finally, in Fig. 9 we compare $\langle F\rangle$ with the displacement $\sqrt{\langle u^2(T)\rangle/a^2}$. Again we see a linear relationship at low T, although important deviations are observed near T_g and T_m. Such behavior can be understood from Eq. (3) by replacing T with $\langle F\rangle$ using Eq. (14),

$$\langle F\rangle = K\sqrt{\langle u^2(T)\rangle}, \tag{15}$$

where K is an effective elastic constant defined as

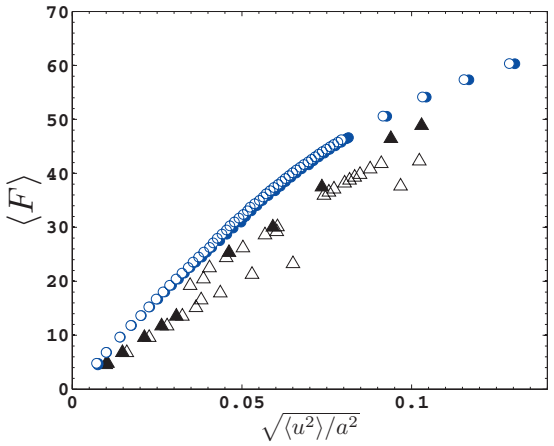

FIG. 9. Average force vs the normalized quadratic mean displacement at $P=30.0$ for crystals (circles) and glasses (triangles) with $N=864$ (filled symbols) and $N=500$ (open symbols). An almost "Hooke law" can be seen at low temperatures.

$$K \equiv m\sqrt{\frac{\langle \omega^2 \rangle}{\langle \omega^{-2} \rangle}}. \tag{16}$$

Equation (15) is basically the Hooke law. The elastic constant is defined through the ratio between the moments of the density of states. Figure 9 shows that the average elastic constant of the glass is lower than in the crystalline case, i.e.,

$$\frac{\langle \omega^2 \rangle_g}{\langle \omega^{-2} \rangle_g} < \frac{\langle \omega^2 \rangle_c}{\langle \omega^{-2} \rangle_c}, \tag{17}$$

where the subindex g is used to denote the glass and c the crystal. Notice that the previous ratio is determined basically by the low frequency anomalies through $\langle \omega^{-2} \rangle$, since according to Eq. (14) and Fig. 8, we have $\langle \omega^2 \rangle_g \simeq \langle \omega^2 \rangle_c$. Anomalies tend to increase $\langle \omega^{-2} \rangle_g$, reducing the average elastic constant. We can close the logic circle by saying that this reduction comes from the low coordination of the glassy network, which produces the boson peak. In fact, in Ref. 22 it was shown that $\langle \omega^{-2} \rangle_c / \langle \omega^{-2} \rangle_g \approx 2/3$. Using this piece of information, we can estimate the ratio between average elastic constants in the glass and in the crystal near T_g,

$$\frac{K_g}{K_c} \approx \sqrt{\frac{2}{3}} \approx 0.82. \tag{18}$$

For example, using the data for $N=864$ atoms from Fig. 9, near T_g for $\sqrt{\langle u^2(T) \rangle / a^2} \approx 0.1$, $\langle F \rangle_c \approx 60$ while $\langle F \rangle_g \approx 49$, which produces a ratio $K_g/K_c \approx 0.81$ close to the proposed value in Eq. (18). The results obtained for $N=500$ atoms have more dispersion. They produce the value $K_g/K_c \approx 0.71$ for the biggest $\sqrt{\langle u^2(T) \rangle / a^2}$.

V. CONCLUSIONS

In conclusion, we have shown that the excess of modes is related with the glass transition by increasing the mean quadratic displacement. Also, we showed that the limit of stability of the solid is roughly given by the Lindemann criteria. A better agreement is obtained by using criteria obtained from density functional theory. Our approach shows that low frequency modes are important to determine T_g. An analysis of the average force shows that the Hooke law is observed for crystals and glasses with a smaller constant in the former case. The ratio between elastic constants can be obtained from the 2/3 ratio between glass transition and melting temperatures. It is in some sense surprising that low frequency modes have an impact upon glass formations, since one can think that near glass transition, modes are excited according to the equipartition of energy and thus all of them are equally important to the mechanical stability of the glass. However, in this article we provided numerical evidence to show that low frequency modes are fundamental to the mechanical stability.[22] In fact, in 1935 Peierls made the observation that the thermodynamical stability of a solid against thermal fluctuations is a subtle matter that concerns dimensionality and LFVMs (Ref. 6) due to the their high population as deduced from the singularity of the Bose–Einstein factor at low frequencies.[22] As a result, crystals in one and two dimensions are unstable against thermal fluctuations, while in three dimensional crystals are stable.[6] Later on, this idea was included in the more general framework of the Mermin–Wigner theorem which concerns order, dimensionality, and Goldstone modes.[49] Some of these ideas are useful in glasses, since they are stable from a laboratory time scale point of view. Once a glass is formed, it must be resistant to the phonon field fluctuations. A limit is thus imposed to the mechanical stability of the glass. Furthermore, for disordered systems, low frequency modes are not only important for their high population but also for their localization properties[22] and crucial effects in thermal equilibrium due to a nonlinear mechanism akin to turbulence.[23]

ACKNOWLEDGMENTS

We thank DGAPA-UNAM (Project Nos. IN-117806 and IN-111906) and CONACyT (Project Nos. 48783-F and 50368). G.G.N. thanks DGAPA-UNAM for a sabbatical scholarship. The calculations were performed at Kanbalam and Bakliz supercomputers at DGSCA-UNAM.

APPENDIX A: LOCAL ENERGY MINIMUMS AND JAMMED STATES

In this appendix, we prove that a system made of soft spheres prepared from a strictly jammed state of hard spheres is in a local energy minimum when the interaction radius is chosen in an appropriate way. The gradient of the potential given by Eq. (8) is

$$\nabla \Phi(\mathbf{r}_1, \ldots, \mathbf{r}_N) = \frac{\beta\epsilon}{\sigma} \sum_{i=1}^{N} \sum_{i<j}^{N} \left(\frac{\sigma}{r_{ij}} \right)^{\beta+1} \mathbf{n}_{ij}, \tag{A1}$$

where $\mathbf{n}_{ij}$ is the unitary vector in the direction $\mathbf{r}_i - \mathbf{r}_j$. Consider a system prepared from a strictly jammed state. If the separation between hard spheres is d and $d=\sigma$, the gradient for the soft sphere glass is

$$\nabla\Phi(\mathbf{r}_1,\ldots,\mathbf{r}_N)=\frac{\beta\epsilon}{\sigma}\sum_{i=1}^{N}\sum_{i<j}^{N}\mathbf{n}_{ij}, \tag{A2}$$

since even if there are many spheres nearly touching each other, the range of the interaction potential is strictly σ and there are no overlaps in the hard-sphere case. For the hard-sphere system, all the forces are equilibrated and one must have

$$\sum_{i=1}^{N}\sum_{i<j}^{N}\mathbf{n}_{ij}=0. \tag{A3}$$

Thus $\nabla\Phi(\mathbf{r}_1,\ldots,\mathbf{r}_N)=0$, and the potential has a minimum for this configuration (or maximum, which is clearly not the case). In our simulations, we found that certain steps were necessary to relax the systems toward the minimum due to the numerical errors, since the cutoff radius needs to be taken equal to the average distance between particles and not all particles are at exactly the same distance.

APPENDIX B: AVERAGE FORCE SCALING WITH THE TEMPERATURE

In this appendix we obtain the relationship between the average force and the temperature. It is worthwhile mentioning that the origin of this scaling validates the use of a harmonic Hamiltonian, since in that case the potential energy can be written as[50]

$$\Phi(Q_1,\ldots,Q_{3N})=\sum_{s=1}^{3N}\frac{\omega_s^2}{2}Q_s^2, \tag{B1}$$

where the Q_s's are the normal mode coordinates. The ν component of the force over particle j is given by

$$F_j^\nu=-\frac{\partial\Phi(\mathbf{r}_1,\ldots,\mathbf{r}_N)}{\partial\mathbf{r}_j^\nu}=-\sum_{s=1}^{3N}\omega_s^2Q_s\frac{\partial Q_s}{\partial\mathbf{r}_j^\nu} \tag{B2}$$

from where we obtain

$$\|F_j\|^2=\sum_{v=1}^{3}F_j^\nu F_j^\nu=\sum_{v=1}^{3}\sum_{s,s'=1}^{3N}\omega_s^2\omega_{s'}^2Q_sQ_{s'}\frac{\partial Q_s}{\partial\mathbf{r}_j^\nu}\frac{\partial Q_{s'}}{\partial\mathbf{r}_j^\nu}. \tag{B3}$$

However, each normal mode coordinate Q_s is a linear combination[50] of the $\mathbf{r}_j$'s,

$$Q_s=\sum_{j,v}u_s^\nu(j)\mathbf{r}_j^\nu,$$

where $u_s^\nu(j)$ are the elements of the matrix which diagonalizes the dynamical matrix generated from $\Phi(\mathbf{r}_1,\ldots,\mathbf{r}_N)$. It follows that

$$\frac{\partial Q_s}{\partial\mathbf{r}_j^\nu}=u_s^\nu(j) \tag{B4}$$

and

$$\|F_j\|^2=\sum_{v=1}^{3}\sum_{s,s'=1}^{3N}\omega_s^2\omega_{s'}^2Q_sQ_{s'}u_s^\nu(j)u_{s'}^\nu(j).$$

Now we sum over sites

$$\sum_{j=1}^{N}\|F_j\|^2=\sum_{s,s'=1}^{3N}\omega_s^2\omega_{s'}^2Q_sQ_{s'}\sum_{j=1}^{N}\sum_{v=1}^{3}u_s^\nu(j)u_{s'}^\nu(j).$$

Due to the orthonormalization properties of the normal modes, the last two sums give a delta $\delta_{s,s'}$

$$\sum_{j=1}^{N}\|F_j\|^2=\sum_{s=1}^{3N}\omega_s^4Q_s^2. \tag{B5}$$

By taking a thermal average and using the equipartition of energy we get,

$$\langle F\rangle=\sqrt{\frac{1}{N}\sum_{s=1}^{3N}\omega_s^4\langle Q_s^2\rangle}=\sqrt{3m\langle\omega^2\rangle k_BT}, \tag{B6}$$

where $\langle\omega^2\rangle$ is the second moment of the density of states,

$$\langle\omega^2\rangle=\frac{1}{3N}\sum_{s=1}^{3N}\omega_s^2=\int_0^\infty\omega^2g(\omega)d\omega.$$

[1] J. Langer, Phys. Today **60** (2), 8 (2007).
[2] P. W. Anderson, Science **267**, 1615 (1995).
[3] J. C. Phillips, Rep. Prog. Phys. **59**, 1133 (1996).
[4] J. Jackle, Rep. Prog. Phys. **49**, 171 (1986).
[5] R. Kerner and J. C. Phillips, Solid State Commun. **117**, 42 (2001).
[6] K. Binder and W. Kob, *Glassy Materials and Disordered Solids* (World Scientific, Singapore, 2005).
[7] W. A. Kamitakahara, R. L. Cappeletti, P. Boolchand, B. Halfpap, F. Gompf, D. A. Neumann, and H. Mutka, Phys. Rev. B **44**, 94 (1991).
[8] P. K. Gupta and J. K. Mauro, J. Chem. Phys. **130**, 094503 (2009).
[9] G. D'Angelo, G. Carini, C. Crupi, M. Koza, G. Tripodo, and C. Vasi, Phys. Rev. B **79**, 014206 (2009).
[10] J. C. Phillips, J. Non-Cryst. Solids **34**, 153 (1979).
[11] M. F. Thorpe, J. Non-Cryst. Solids **57**, 355 (1983).
[12] C. A. Angell, J. Phys.: Condens. Matter **16**, S5153 (2004).
[13] G. G. Naumis, Phys. Rev. B **61**, R9205 (2000).
[14] D. Selvanathan, W. J. Bresser, and P. Boolchand, Phys. Rev. B **61**, 15061 (2000).
[15] Y. Wang, J. Wells, D. G. Georgiev, P. Boolchand, K. Jackson, and M. Micoulaut, Phys. Rev. Lett. **87**, 185503 (2001).
[16] D. Novita, P. Boolchand, M. Malki, and M. Micoulaut, Phys. Rev. Lett. **98**, 195501 (2007).
[17] M. Wyart, Ann. Phys. (Paris) **30**, 1 (2005).
[18] A. J. Liu and S. R. Nagel, Nature (London) **396**, 21 (1998).
[19] P. G. Debenedetti, *Metastable Liquids* (Princeton University Press, Princeton, 1996).
[20] G. G. Naumis, Phys. Rev. B **73**, 172202 (2006).
[21] G. G. Naumis, J. Non-Cryst. Solids **352**, 4865–4870 (2006).
[22] G. G. Naumis and H. Flores-Ruiz, Phys. Rev. B **78**, 094203 (2008).
[23] J. R. Romero-Arias and G. G. Naumis, Phys. Rev. E **77**, 061504 (2008).
[24] A. Huerta and G. G. Naumis, Phys. Lett. A **299**, 660 (2002).
[25] A. Huerta and G. G. Naumis, Phys. Rev. Lett. **90**, 145701 (2003).
[26] A. Huerta, G. G. Naumis, D. T. Wasan, D. Henderson, and A. Trokhymchuk, J. Chem. Phys. **120**, 1506 (2004).
[27] A. Huerta and G. G. Naumis, Phys. Rev. B **66**, 184204 (2002).
[28] G. G. Naumis, Phys. Rev. E **71**, 026114 (2005).
[29] M. Wyart, S. R. Nagel, and T. A. Witten, Europhys. Lett. **72**, 486 (2005).
[30] C. Brito and M. Wyart, Europhys. Lett. **76**, 149 (2006).
[31] N. Xu, M. Wyart, A. J. Liu, and S. R. Nagel, Phys. Rev. Lett. **98**, 175502 (2007).
[32] K. Lu, E. E. Brodsky, and H. P. Kavehpour, Nat. Phys. **4**, 404 (2008).
[33] W. A. Phillips, U. Buchenau, N. Nücker, A. J. Dianoux, and W. Petry, Phys. Rev. Lett. **63**, 2381 (1989).
[34] U. Buchenau and R. Zorn, Europhys. Lett. **18**, 523 (1992).
[35] D. Engberg, A. Wischnewski, U. Buchenau, L. Börjesson, A. J. Dianoux, A. P. Sokolov, and L. M. Torell, Phys. Rev. B **58**, 9087 (1998).
[36] B. Frick and D. Richter, Phys. Rev. B **47**, 14795 (1993).

[37] K. L. Ngai, J. Non-Cryst. Solids **275**, 7 (2000).
[38] P. G. Debenedetti and F. H. Stillinger, Nature (London) **410**, 259 (2001).
[39] S. V. Nemilov, *Thermodynamic and Kinetic Aspects of the Vitreous State* (CRC, Boca Raton, 1994).
[40] R. W. Hall and P. G. Wolynes, J. Chem. Phys. **86**, 2943 (1987).
[41] A. Donev, S. Torquato, F. H. Stillinger, and R. Conelly, J. Appl. Phys. **95**, 989 (2004).
[42] S. V. Meshkov, Phys. Rev. B **55**, 12113 (1997).
[43] L. Berthier and T. A. Witten, Europhys. Lett. **86**, 10001 (2009).
[44] J. Q. Broughton and G. H. Gilmer, J. Chem. Phys. **79**, 5095 (1983).
[45] C. Brito and M. Wyart, J. Stat. Mech.: Theory Exp. **08**, L08003 (2007).
[46] Y. Asano and K. Fuchizaki, J. Phys. Soc. Jpn. **78**, 055002 (2009).
[47] E. A. Mastny and J. J. de Pablo, J. Chem. Phys. **127**, 104504 (2007).
[48] V. Mazzacurati, G. Ruocco, and M. Sampoli, Europhys. Lett. **34**, 681 (1996).
[49] P. M. Chaikin and T. C. Lubensky, *Principles of Condensed Matter Physics* (Cambridge University Press, Cambridge, 2000).
[50] H. Goldstein, *Classical Mechanics* (Addison-Wesley, Reading, 1959).